JOURNAL OF MATERIALS SCIENCE 32 (1997) 6317–6323

The fractal geometry of Si_3N_4 wear and fracture surfaces

Z. CHEN, J. J. MECHOLSKY Jr, T. JOSEPH and C. L. BEATTY
Department of Materials Science and Engineering, University of Florida, Gainesville, FL 32611, USA

Good mechanical properties and chemical stability at high temperatures make silicon nitride a good candidate as an advanced engine material. Much research has been done to characterize the mechanical strength and resistance of crack propagation in this material. In this paper, we use fractal analysis to study the geometry of Si_3N_4 fracture and wear surfaces. We found that the geometries of the failure surfaces as characterized by the fractal dimensional increment, D^*, under different failure stress states are similar for the same brittle material, but different for different brittle materials. The similar D^* in an identical brittle material implies that the failure process in the material is the same regardless of loading mode, i.e., mode I or mixed-mode stress. The fractal technique is shown to be useful for correlating the fractal dimension to the material properties and fracture-surface topography.

1. Introduction

Silicon nitride has very good mechanical properties and good chemical stability at high temperatures. These properties make silicon nitride a candidate for advanced engine material. Much research has been done to characterize the mechanical strength and resistance to crack propagation and fracture [1–3]. Since most ceramic components are designed to sustain a complex stress state during their applications, we wish to determine whether or not there is substantial difference in the fracture surfaces fractured under different stress states such as simple tensile, flexural or complex stresses. There have been few studies reported with regard to quantitative descriptions of the geometry of Si_3N_4 fracture surfaces which are formed under different stresses. In this study, we use fractal analysis to describe quantitatively the geometry of different Si_3N_4 fracture surfaces.

2. The geometry of failure surfaces

The fracture process in brittle materials leaves characteristic markings on the fracture surface. The importance of these markings on the fracture surfaces of brittle materials was recognized in terms of quantitatively identifying characteristic parameters such as the stress at fracture and velocity of the crack front [4, 5]. An idealized fracture surface contains an origin with surrounding topography showing mirror, mist and hackle regions and often macroscopic crack branching (Fig. 1). Building on the work of Griffith, Irwin [6] introduced the concept of the stress intensity factor, K_I, and developed the field of linear elastic fracture mechanics (LEFM). We generally evaluate the critical stress intensity factor, K_{Ic}, i.e., the resistance to fracture, as

$$K_{Ic} = Y\sigma c^{1/2} \quad (1)$$

where Y is a "constant" dependent on the geometry and location of the crack as well as the loading configuration; σ and c are the stress and crack size at fracture, respectively.

However, not all fracture surfaces show the idealized features. In Fig. 2, four Si_3N_4 fracture surfaces (formed from an identical material) show apparently different appearances. The appearances of fracture surfaces are determined not only by material properties but also by the initial flaw or defect sizes and applied stress states. The appearance of the fracture surface is an extrinsic phenomenon and different workers can give the surface different descriptions under different observation environments such as light direction, light intensity, or type of light. However, the geometry of the fracture surface can be described quantitatively and represents the nature of fracture surface formation.

Since fracture in brittle materials is an atomic-bond-breaking process, there could exist a relationship between the type of bond breaking and its fracture surface geometry. Recent developments in fractal geometry and the techniques of fractal dimension measurement on fracture surfaces have presented the possibility of linking fractal geometry of fracture surfaces to the type of materials being fractured [7–9].

Many researchers have shown that the nature of the fracture surface can be described using fractal geometry [10–16]. Fractal geometry is a non-Euclidean geometry that allows for non-integer dimensions

0022–2461

and has been used to describe a variety of natural processes [10]. The fractal dimension of a line, for example, will reside between one and two. A "smooth" line would have a dimension of one (Euclidean). A tortuous line would have a dimension greater than one. The dimension increases as the tortuosity increases. The fractal dimension of a surface lies between two and three, etc.

Mecholsky and co-workers [8, 9, 12, 14] and Mackin [13] experimentally determined a relationship between fracture toughness, K_{Ic}, and fractal dimension, D. They found that

$$K_{Ic} = Ea_0^{1/2}D^{*1/2} + K_0 \quad (2)$$

where E is the elastic modulus, D^* is the fractal dimensional increment and a_0 is a characteristic atomic dimension. K_0 accommodates the possibility of perfectly plane fracture, i.e., $D = 2$, and is close to zero for many ceramics [7, 12, 14]. In order to define a_0 better, it is useful to rearrange Equation 2. On the assumption of plane-stress conditions for simplicity, it can be shown [7] that

$$a_0 = \frac{2\gamma}{ED^*} \quad (3)$$

where γ is the fracture energy and can be expressed as $K_{Ic}^2/2E$. The value of a_0 has been evaluated for many materials [7, 12, 14]. The range of a_0 is from a few ångströms to tens of ångströms in inorganic materials. a_0 is thought to be a material characteristic which is related to stretching ability of the atomic or molecular bond near the crack tip. For example, a_0 could be the length of a stretched lattice distance in single crystals, the size of the "hole" in a disordered molecular amorphous arrangement, or the process zone size in polycrystalline materials. a_0 depends on material microstructure and atomic structure. Equation 3, then, provides a link between the material's toughness, fracture surface geometry and atomic structure.

On the basis of previous work, we thought that the study of fractal geometry on silicon nitride surfaces could provide additional information to help us to understand the process of silicon nitride fracture or mechanical failure.

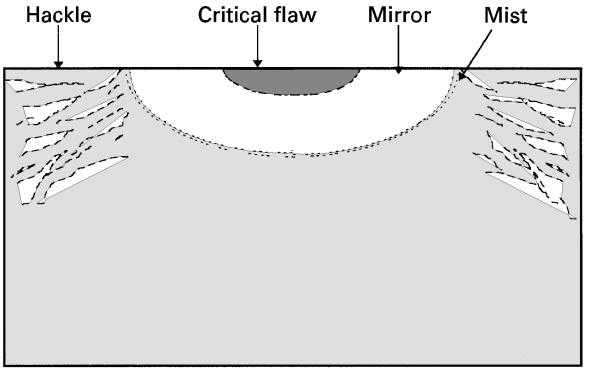

Figure 1 Schematic diagram showing typical brittle fracture surface characteristics: critical flaw, mirror, mist and hackle.

3. Experimental procedure

Commercial (Toshiba) hot isostatically pressed silicon nitride bearing ball material was used for this study. Four types of fracture surfaces were analysed in the experiment. Three fracture surfaces and one wear surface are shown in Fig. 2. Sample I was a bearing ball which was damaged during a bearing test under about 3.3 GPa maximum contact stress. Samples II and III were fractured at different stresses (402 MPa for sample II and 216 MPa for sample III) under four-point flexure. Sample IV was fractured at a maximum tensile stress of 800 MPa during a rotating-cantilever-beam fatigue test. Three typical locations A, B and

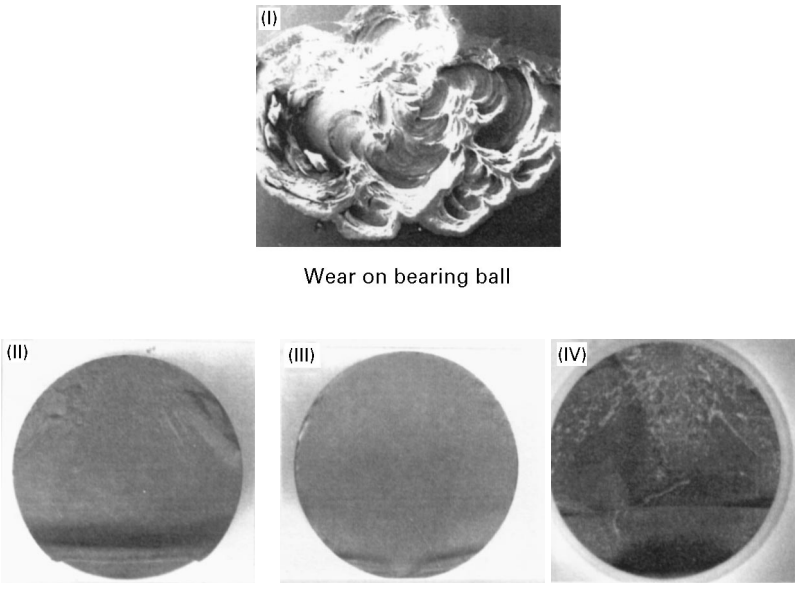

Figure 2 Samples I, II, III and IV are from the same material (type A). Sample I failed during a bearing test. Samples II and III fractured in bending at different stresses. Sample IV was fractured during a rotating fatigue test. Each case resulted in the characteristic markings on the surface.

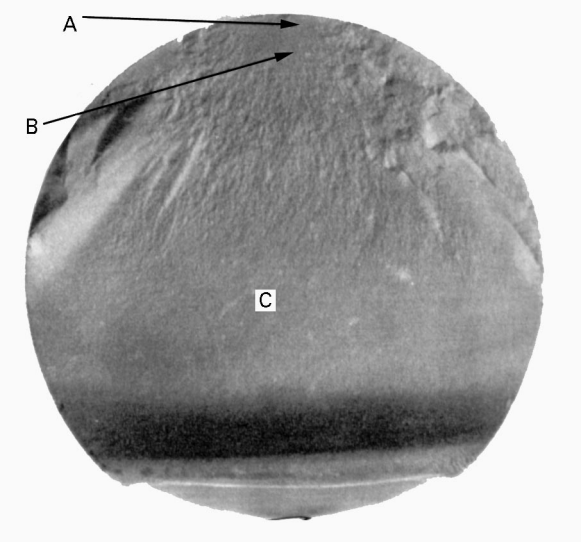

Figure 3 Fractal dimensions were measured from the locations A ($D^* = 0.33$), B ($D^* = 0.34$) and C ($D^* = 0.32$), respectively.

C on sample II's fracture surface, which correspond to the mirror, mist and initially compressive region (Fig. 3), also were investigated by measuring their fractal dimensions in order to determine whether the fractal dimension is independent of the location on the fracture surface.

Two different techniques were used to measure experimentally the fractal dimension: a polishing method, i.e., the slit island analysis (SIA), and the atomic force microscopy (AFM) method. The fractal dimensions of the failure surfaces were determined using SIA on portions of "island" contours of the fracture surface and the Richardson (perimeter-ruler length) method on the island contours [10, 13]. The first technique uses dental impression material to create a negative replica of the fracture surface. After the replica dries, a positive of the fracture surface is made by filling the cavity formed in the impression material with epoxy. After the epoxy is cured, the positive impression is coated with an electroless nickel plating. The coated sample is then covered by epoxy. The replica is now treated in the usual manner [8, 13] to produce slit island contours by polishing approximately parallel to the fracture surface (Fig. 4). The length of a section of the perimeter of the island, L, is a function of the size of the ruler unit, r, selected, such that

$$L = kr^{-D^*} \tag{4}$$

where k is a constant and D^* is the fractal dimensional increment. Note that, for Euclidean objects, $D^* = 0$ and L is a constant. Also note that, as r increases, i.e., your measurement ruler scale becomes larger, the length measured is smaller. Conversely, the finer the measuring ruler, the longer is the length. The details of this process were described by Plaia and Mecholsky [14].

The second technique uses AFM (TopoMetrix, Santa Clara, CA). The basic components of an atomic force microscope are shown in Fig. 5. The cantilever beam keeps a constant distance between the tip and

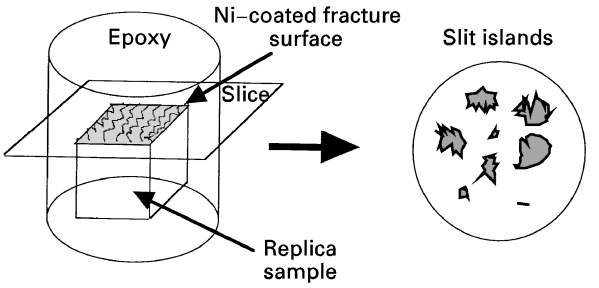

Figure 4 Schematic diagram showing the slit islands of the fracture surface obtained using the SIA technique.

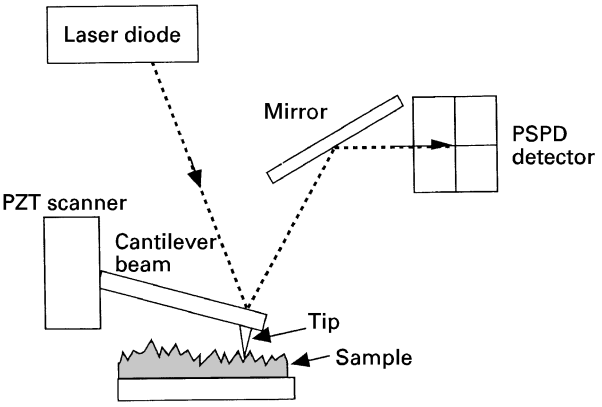

Figure 5 Schematic diagram showing the basic components of the atomic force microscope.

fracture surface by control of the beam angle. The distance between the tip and the surface is determined by the atomic forces between these two materials. A feedback loop is established to maintain the constant distance. When the cantilever moves on the x–y plane with a subångström resolution controlled by a piezoelectric ceramic transducer (PZT), the change in the surface profile is measured using a photosensitive position displacement (PSPD) detector by recording the angle change of the reflected laser beam from the cantilever beam. The atomic force microscope scanner range is 50 μm. A silicon nitride tip was supplied by Topometrix with a tip diameter of less than 40 nm. The data are stored electronically and then a three-dimensional (3D) fracture surface image is created directly from the data by TOPOMETRIX SPM V 2.3 software. Another software module then sections the 3D fracture surface image at different altitudes (different Z levels) parallel to the fracture surface. This sectioning forms "slit islands" from which the fractal dimension is obtained using a box-counting method [10]. The value of the fractal dimension from a 20 μm × 29 μm measured region is averaged from 12 fractal data measured at different Z levels.

Fracture surfaces, fatigue fracture surfaces and wear surfaces were used in this experiment to investigate whether the fracture surface geometry is stress state dependent or material dependent, i.e. material bond type dependent.

In order to determine whether the fracture surface geometry is dependent on the stress state or on the

TABLE I Fractal dimensional increment D^* data where D_1^* and D_2^* are obtained from the polishing method and the AFM method, D^* is the average value and $\pm$ indicates the standard deviation

	Surface I	Surface II	Surface III	Surface IV	Location A	Location B	Location C
D_1^*	0	0.32 ± 0.03	0.33 ± 0.03	0.33 ± 0.04	0	0	0
D_2^*	0.31 ± 0.05	0.33 ± 0.05	0.34 ± 0.03	0.30 ± 0.05	0.33 ± 0.04	0.34 ± 0.03	0.32 ± 0.03
D^*	0.31	0.33	0.34	0.32	0.33	0.34	0.32

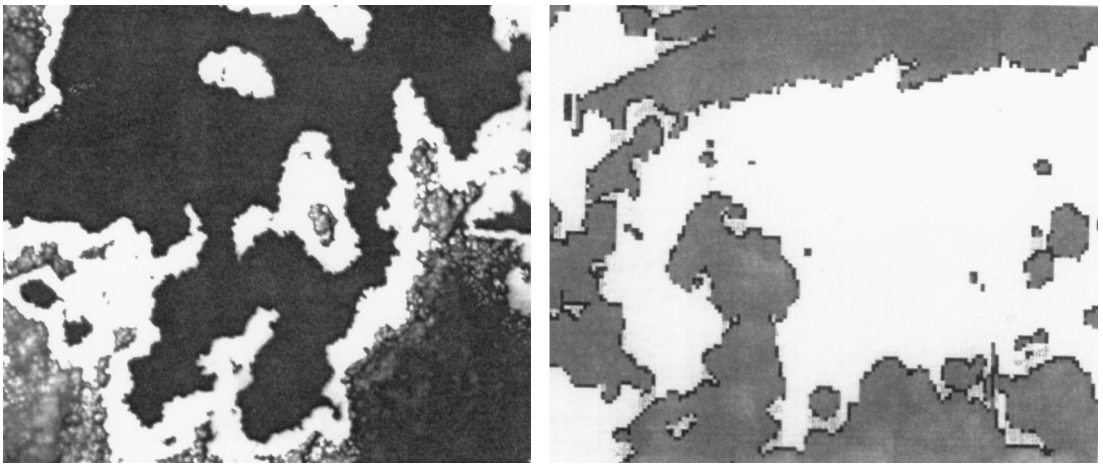

Figure 6 Slit island contours are shown in this photograph. On the left, the contour at $\times 100$ ($D^* = 0.33$) was produced using the SIA method. The right was obtained by AFM at $\times 3200$ ($D^* = 0.34$). The two photographs are similar regardless of the different scales.

type of material bond, two facts have to be determined. One is whether D^* is independent of the fracture surface location; the other is whether D^* data from the AFM measurement represent D^* data from traditional methods, such as the SIA method. We measured the fractal dimension, D^*, from different locations on sample II (Fig. 2). If the results show that D^* is independent of the locations on the surface, then we can measure D^* from the smooth (mirror) region to represent the D^* values for the rest of the samples. Doing this not only can save tremendous time but also can make for easy AFM scanning. It is much easier to scan on a region with less tortuosity. If the results show that D^* is dependent on the surface locations, then D^* has to be measured on different locations for each sample before any conclusions can be made in this study. We also measured D^* from samples II and III using both methods, i.e., the SIA method and the AFM method, for comparison purposes.

4. Results and discussion

A summary of fractal dimension data in the form of D^* for different samples shown in Fig. 2 is presented in Table 1. The results show that for the different locations A, B and C on the fracture surface (sample II) the fractal dimensions (Fig. 3) are statistically the same, which indicates that D^* is independent of the fracture surface location. At first, the constant D^* value may seem contradictory to our observations because the surface has obviously different roughness levels at the three different locations. However, even though the absolute roughness values are different, the fractal dimension, as characterized by the fractal dimensional increment, D^*, is the same because D^* is the slope of different length measurements corresponding to different ruler lengths (Equation 4). Although the surface is rougher in one part than the other, the relative changes in tortuosity are the same in the three regions. The visual appearance, at relatively low magnifications, of the apparently smooth regions, e.g., in C, means that the perturbations revealed using AFM are smaller than the wavelength of light, and really are not smooth.

Fig. 6 shows examples of fracture contours from both the SIA method and the AFM method. The D^* data from both measuring methods show reasonable consistency (Table I), which further indicates that AFM is an acceptable method for measuring D^* from the fracture surface. The AFM and SIA techniques measure D^* at different scales. The macroscopic SIA method cannot accurately measure the "C" region in Fig. 3 because it is not sensitive enough with the polishing technique that was used here. This lack of measurement ability does not mean that the region is smooth, just that a more sensitive method must be used to measure the appropriate roughness. Therefore, most data that we show in the following sections were measured using the AFM method.

D^* data from all the fracture surfaces shown in Table I indicate several interesting phenomena, such as similar D^* values from the different failure surfaces, the relationship between K_{Ic} and D^* shown later in Fig. 8, and the atomic or molecular bond size values of a_0. We shall discuss each of these phenomena in the following sections.

4.1. D^* values from different failure surfaces

Three fracture surfaces and one wear surface have similar fractal dimensions, D^*, regardless of their apparently different surface appearances and fracture stress states. The fractal dimension D^* values obtained are given in Table I. The fractal dimension for each surface was averaged from 12 measurements. The typical D^* data distribution from one surface is displayed in Fig. 7. There is no systematic variation in D^* from near the origin to beyond the crack branching region. Thus, we conclude that D^* is a constant value for all regions.

Of course in some materials there may be more than one value for the fractal dimension in different regions, i.e., multifractal materials [17]. In single crystals and glasses, we would not expect to measure multifractals and, indeed, do not [7]. We should expect to see multifractals in composites and multiphase materials such as cement and geological materials and, indeed, do [18]. Fine-grained polycrystalline materials could either be multifractal or single valued depending on the material structure at all length scales and the mechanism of fracture. In this particular case, this silicon nitride bearing ball material appears to have a single fractal dimension in all regions and at all scale lengths.

The D^* values from these silicon nitride surfaces indicate that the geometry of silicon nitride fracture surfaces are fractal. Two silicon nitride fracture contours for different magnifications show the nature of the fractal scaling, i.e., self-similarity (Fig. 6). There is some controversy in the literature about the nature of fracture surfaces [7, 16, 17, 19, 20], i.e., whether or not they are self-similar or self-affine. A self-similar surface is one in which the scaling is isotropic. A self-affine surface is one in which the scaling parameter is a vector quantity. We think that there are some fracture surfaces which are self-similar and some which are self-affine. Fracture surfaces which are formed in materials which are isotropic should be self-similar, e.g., glasses and fine-grained polycrystalline brittle materials [7]. Natural and man-made composites can be either self-similar or self-affine. Cements and geological materials, such as westerly granite, would be expected to be self-affine [18]. From the data presented, it appears that this silicon nitride material fractures in a self-similar manner.

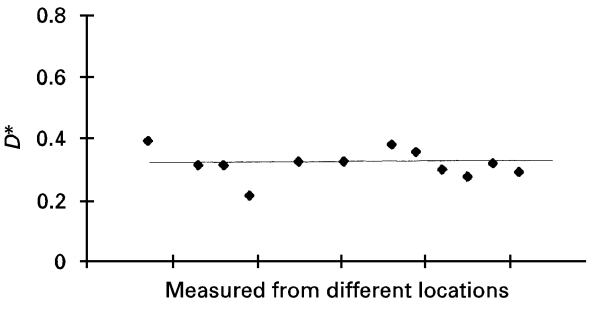

Figure 7 Typical distribution of the measured fractal dimensional increment, D^*; data were from one fracture surface using AFM. $D^*_{avg} = 0.32$.

In addition, the same D^* value regardless of stress state, such as pure bending, mixed-mode loading and contact loading, suggests that the failure process in this material is controlled by a common local mechanism such as a type of atomic level mode I stress. In other words, the bond stretches and breaks in a line and can be considered a tensile failure. Other modes may contribute to the rotation of the bonds or the creation of friction on fracture surfaces but do not contribute to the material bond breakage. In other work reported in a separate paper [21], we show that the crack path under a complex stress state such as Hertzian contact loading follows a mode I stress path. Singh and Shetty [22] also point out in their research on similar materials that a mode I stress controls the crack path when the initial crack is loaded under a mixed-mode stress. From a failure surface geometry perspective, the fact of similar D^* values on the different failure surfaces implies that failure in these brittle materials is caused by a similar: process mode I stress. In other words, the fractal dimension D^* may be an indication of a failure process in brittle materials.

4.2. The relation between D^* and K_{Ic}

If the results in Section 4.1 are true, i.e., the similarity of D^* values represent a similar failure process in brittle materials caused by a local mode I stress, then there should exist a relation between D^* and K_{Ic}. The data on K_{Ic} versus $D^{*1/2}$ is plotted with other polycrystalline material data (Table II [23]) in Fig. 8, where the silicon nitride K_{Ic} used is taken from its large-crack R-curve value ($K_{Ic} = 5.4$ MPa $m^{1/2}$) [24]. The K_{Ic} versus $D^{*1/2}$ values lie approximately on a straight line with the value of K_0 approximately zero. This indicates that the Si_3N_4 data are consistent with the relationship between K_{Ic} and D^* (Equation 2), which was proposed by Mecholsky and co-workers [8, 9, 12, 14] and Mackin [13]. Thus, as the fractal dimension increases, the value of the critical stress intensity factor, K_{Ic}, increases. This result further implies that the failure surface geometry can reflect the strength of the material's bonding, i.e., the higher the strength of the bond, the more tortuous is the surface geometry.

TABLE II The data on fracture toughness and fractal dimensional increment of brittle polycrystalline materials

Number	Material	K_{Ic} (MPa $m^{1/2}$)	D^*
1	Zinc silicate (ZSGC No. 1)	2.0	0.05
2	Zinc silicate (MS 498-5)	2.2	0.07
3	Zinc silicate (ZSGC No. 2)	2.0	0.09
4	Zinc silicate (MS 500-4)	2.2	0.12
5	Al_2O_3 (UCC)	4.0	0.15
6	Pyroceram (9606)	2.5	0.17
7	Al_2O_3 (WESGO A 1500)	3.6	0.20
8	Al_2O_3 (AD99)	2.9	0.21
9	Al_2O_3 (GEND)	3.9	0.23
10	Al_2O_3 (AD999)	3.9	0.31
11	Al_2O_3 (Lucalox)	4.0	0.31
12	Si_3N_4	5.4	0.34

4.3. The relation between the a_0 spacing and K_{Ic} values

Based on previous studies, a_0 is defined as the "unit process" of fracture [7, 12, 14, 23], which can be interpreted as a process zone near the crack tip on the atomic scale. Silicon nitride material, with its rod-like microstructure (Fig. 9) exhibits *R*-curve behaviour, i.e., K_{Ic} increases as the crack length increases. In other words, the process zone around the crack tip increases in the range of the size of the microstructure as the crack size increases, as has been observed and discussed by many workers [25, 26]. We found that the process zone in the range of the atomic scale, which can be represented by a_0, also shows an increase as the crack size increases (Fig. 10). The range of a_0, which is calculated from Equation 3, is in the range from the length of the molecular bond to the size of the "hole" in inorganic amorphous materials (from 3.3 to 11.4 Å) [27]. A fractographic study of the fracture surfaces indicates that the fracture of Si_3N_4 is governed by intergranular fracture, and the grain boundary phase in the silicon nitride has been identified as amorphous [28]. We think that the increase in a_0 could be attributed to an increase in the process zone from the stretching bond length (3.3 Å) to the size of the "hole" (11.4 Å) in the amorphous grain boundaries. Defining an experiment to determine the stretching bond length or the hole size under stress just before fracture is difficult. However, the sizes of a_0 can be calculated from the fractal dimension, D^*, measurements and this calculation shows them to be within the range expected [29].

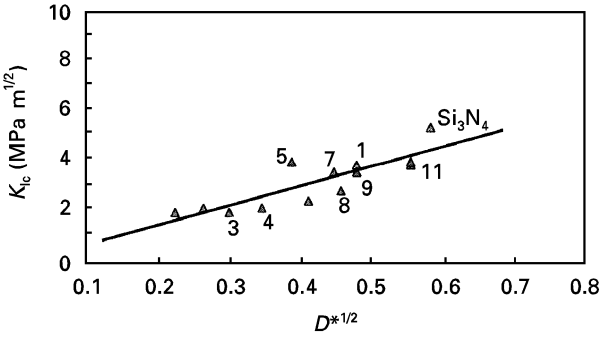

Figure 8 The toughness of polycrystalline ceramics as a function of D^*. The numbers correspond to those in Table II.

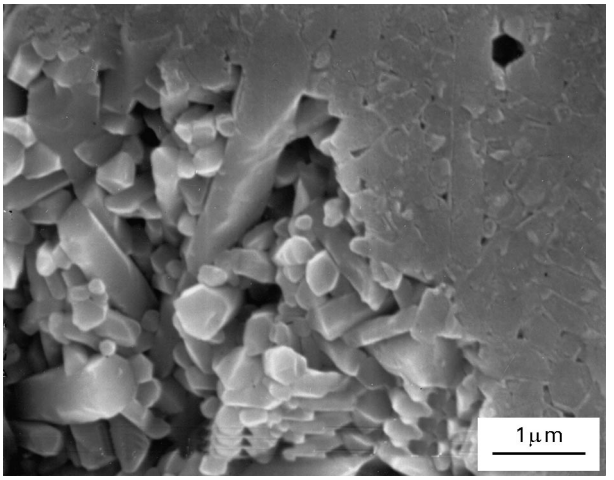

Figure 9 Scanning electron micrograph showing the rod-like grain structure of Si_3N_4.

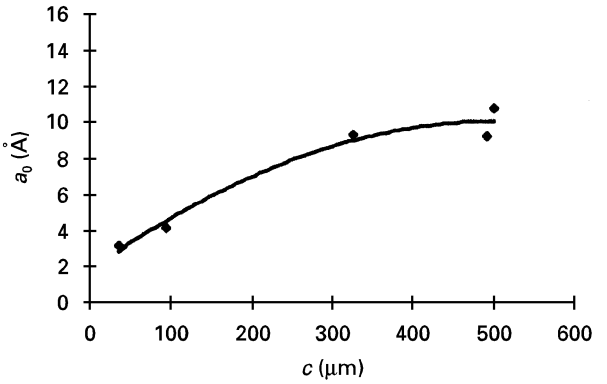

Figure 10 An increase in a_0 spacing with initial crack size implies an *R*-curve behaviour of Si_3N_4 on an atomic scale.

5. Conclusions

This study showed that for one material (Si_3N_4) the fractal dimension, D^*, is the same for failure surfaces created under different stress states. This implies that the fracture process in brittle materials could be controlled by one stress mode, such as a local mode I stress. The existence of the relation between D^* and the critical stress intensity factor, K_{Ic} (Equation 2), for Si_3N_4 further supports this supposition. Furthermore, the D^* value is independent of scaling factors for an identical material and again demonstrates the fractal nature of fracture surfaces. The a_0 spacing calculated from Equation 3 is thought to be an atomic-scale process zone near the crack tip and is an indication of the reaction of the grain-boundary phase to the *R*-curve behaviour of the silicon nitride at the atomic scale.

The information from this study implies that

(i) the fractal dimension of the fracture surface provides additional information to indicate that the brittle material failure process is governed by local bond breaking and controlled by a mode I type of stress regardless of the global stress state,
(ii) the fracture process in Si_3N_4 is a self-similar process from small scales to large scales, represented by its fractal dimension,
(iii) the relationship between D^* and the material constants further implies that fracture is a fractal process and
(iv) using the relation of the fractal dimension and fracture energy we show an atomic-scale process zone near the crack tip.

The reason that the fractal approach is appealing is that it not only provides a means of characterizing the material's failure surface but also suggests a means for generation of the fracture surface. From this study, the fractal method emerges as a method with potential for identification of a failure model and eventually will lead to an understanding of fracture and wear processes in material structures.

References

1. S. W. FREIMAN, A. WILLIAMS, J. J. MECHOLSKY and R. W. RICE, in "Ceramic Microstructures' 76", 1976, edited by R. M. Fulrath and J. A. Pask (Westview Press, Boulder, CO, 1977).
2. R. W. RICE, K. R. McKINNEY, C. C. WU and S. W. FREIMAN, *J. Mater. Sci.* **20** (1985) 1392.
3. M. G. JENKINS, M. K. FERBER and C. K. LIN, *J. Amer. Ceram. Soc.* **76** (1993) 788.
4. E. B. SHAND, *J. Am. Ceram. Soc.* **42** (1959) 474.
5. E. F. PONCELET, *Trans. Soc. Glass Technol.* **52** (1958) 279.
6. G. R. IRWIN, Sagamore Research Conference Proceedings, 1956, Vol. 2, pp. 289–305.
7. J. J. MECHOLSKY Jr., in "Fractography of Glasses and Ceramics III,"Ceramic Transactions, Vol. 64, edited by J. R. Varner, V. D. Frechette and G. D. Quinn (The American Ceramic Society, Westerville, OH, 1996).
8. J. J. MECHOLSKY, D. E. PASSOJA and K. S. FEINBERG-RINGEL, *J. Amer. Ceram. Soc.* **72** (1989) 60.
9. J. J. MECHOLSKY, *J. Amer. Ceram. Soc.* **74** (1991) 3136.
10. B. B. MANDELBROT, "The Fractal Geometry of Nature" (Freeman, San Francisco, CA, 1982).
11. B. B. MANDELBROT, D. E. PASSOJA and A. J. PAULLAY, *Nature* **308** (1984) 721.
12. J. J. MECHOLSKY and S. W. FREIMAN, *J. Amer. Ceram. Soc.* **74** (1991) 3136.
13. T. J. MACKIN, PhD thesis, The Pennsylvania State University, University Park, PA.
14. J. J. MECHOLSKY and J. R. PLAIA, *J. Non-Cryst. Solids* **146** (1992) 249.
15. Y. FAHMY, J. C. RUSS and C. C. KOCH, *J. Mater. Sci.* **6** (1991) 1856.
16. E. BOUCHAUD, G. LAPASSET, J. PLANES and S. NAVEOS, *Phys. Rev. B* (1995).
17. S. ROUX and A. HANSEN, in "Disorder and Fracture" edited by J. C. Charmet, S. Roux and E. Guyon (Plenum, New York, 1990).
18. P. A. SCOTT, T. ENGELDER and J. J. MECHOLSKY Jr, in "Fault Mechanics and Transport Property of Rocks", edited by B. Evans and T. Wong (Academic Press, New York, 1992).
19. A. V. NEIMARK, *Phys. Rev. B* **50** (1994) 435.
20. C. Y. POON, R. S. SAYLES and T. A. JONES, *J. Phys.* D **25** (1992) 1269.
21. Z. CHEN, J. C. CUNEO, J. J. MECHOLSKY, Jr. and S. HU, *Wear* **198** (1996) 197–207.
22. D. SINGH and D. SHETTY, *J. Amer. Ceram. Soc.* **72** (1989) 78.
23. J. J. MECHOLSKY Jr, in "Fractography of Glasses and Ceramics II," Ceramic Transactions, Vol. 17, edited by V. D. Frechette and J. R. Varner (American Ceramic Society, Westerville, OH, 1991), pp. 413–52.
24. Z. CHEN and J. J. MECHOLSKY (1997) submitted.
25. J. JOHNSON and D. HOLLOWAY, *Phil. Mag.* (1951) 731.
26. C. LI, D. LEE and S. LUI, *J. Amer. Ceram. Soc.* **75** (1992) 177.
27. J. ZARZYCKI, "Glasses and the Vitreous State" (Cambridge University Press, Cambridge, Cambs., 1991).
28. Z. CHEN and J. J. MECHOLSKY (1997) submitted.
29. J. H. SIMMONS, T. P. SWILER and R. OCHOA, *J. Non-Cryst. Solids* **134** (1991) 179.

Received 7 September 1995
and accepted 4 September 1996